

~~CONFIDENTIAL~~UNCLASSIFIED Copy No.
RM No. L9B25

~~11155~~
NACA
65A006/1

RESEARCH MEMORANDUM

AERODYNAMIC CHARACTERISTICS OF A WING WITH QUARTER-CHORD LINE

SWEPT BACK 35° , ASPECT RATIO 4, TAPER RATIO 0.6,
AND NACA 65A006 AIRFOIL SECTION.

TRANSONIC-BUMP METHOD

By

William C. Sleeman, Jr. and Robert E. Becht

Langley Aeronautical Laboratory
Langley Air Force Base, Va.

CLASSIFIED DOCUMENT

CLASSIFICATION CANCELLED

This document contains classified information affecting the National Defense of the United States within the meaning of the Espionage Laws, USC 5011 and 5012. Its transmission or the revelation of its contents in any manner to an unauthorized person is prohibited by law. Information so classified may be imparted only to persons in the military and naval services of the United States, appropriate civilian officers and employees of the Federal Government who have a legitimate interest therein, and to United States citizens of known loyalty and discretion who of necessity must be informed thereof.

Doc 27 2424 Date 8/18/54

2/24 8/31/54 See

NATIONAL ADVISORY COMMITTEE
FOR AERONAUTICS

WASHINGTON
April 21, 1949

~~CONFIDENTIAL~~

UNCLASSIFIED



UNCLASSIFIED

NATIONAL ADVISORY COMMITTEE FOR AERONAUTICS

RESEARCH MEMORANDUM

AERODYNAMIC CHARACTERISTICS OF A WING WITH QUARTER-CHORD LINE

SWEEP BACK 35° , ASPECT RATIO 4, TAPER RATIO 0.6,

AND NACA 65A006 AIRFOIL SECTION

TRANSONIC-BUMP METHOD

By William C. Sleeman, Jr. and Robert E. Becht

SUMMARY

As part of an NACA transonic research program, a series of wing-body combinations are being investigated in the Langley high-speed 7- by 10-foot tunnel over a Mach number range of 0.60 to 1.18 utilizing the transonic bump.

This paper presents the results of the investigation of a wing-alone and a wing-fuselage combination employing a wing with the quarter-chord line swept back 35° , aspect ratio 4, taper ratio 0.6, and an NACA 65A006 airfoil section. Lift, drag, pitching moment, and root bending moment were obtained for the wing-alone and wing-body configurations. Effective downwash angles and dynamic-pressure characteristics in the region of a probable tail location were also obtained for these configurations and are presented for a range of tail heights at one tail length. In order to expedite publishing of these data, only a brief analysis is included.

INTRODUCTION

The urgent need for aerodynamic design data in the transonic speed range has led to the establishment of a special NACA committee for transonic research. As part of the NACA transonic research program recommended by this committee a series of wing-body configurations having wing plan form as the chief variable are being investigated in the Langley high-speed 7- by 10-foot tunnel utilizing the transonic-bump test technique. For each wing-fuselage combination investigated the lift, drag, pitching moment, and root bending moment characteristics are determined over a Mach number range of 0.60 to 1.18. In addition, effective downwash angles and dynamic-pressure characteristics are obtained for a range of tail heights at one tail length.

~~CONFIDENTIAL~~

UNCLASSIFIED

This paper presents the results of the investigation of the wing-alone and wing-fuselage combinations employing a wing with the quarter-chord line swept back 35° , aspect ratio 4, taper ratio 0.6, and an NACA 65A006 airfoil section.

MODEL AND APPARATUS

The wing of the semispan model had 35° of sweepback referred to the quarter-chord line, a taper ratio of 0.60, aspect ratio of 4, and an NACA 65A006 airfoil section parallel to the free stream. The wing was made of beryllium copper and the fuselage of brass. A two-view drawing of the model is presented in figure 1 while ordinates of the fuselage of fineness ratio 10 can be found in table I.

The model was mounted on an electrical strain-gage balance, which was enclosed in the bump, and the lift, drag, pitching moment, and bending moment about the model plane of symmetry were measured with calibrated galvanometers. The angle of attack was changed with a small electric motor and the value of the angle was determined with a calibrated slide-wire potentiometer.

Effective downwash angles were determined for a range of tail heights by measuring the floating angles of five free-floating tails with the aid of calibrated slide-wire potentiometers. Details of the floating tails are shown in figures 2 and 3, while a photograph of the test setup on the bump, showing the floating tail mounted in the fuselage, is given in figure 4. The tails used in this investigation were the same as those used in the investigation reported in reference 1.

A total-head comb was used to determine dynamic-pressure ratios for a range of tail heights in a plane which contained the 25-percent mean-aerodynamic-chord point of the free-floating tails. The total-head tubes were spaced 0.25 inch apart.

SYMBOLS

C_L	lift coefficient $\left(\frac{\text{Twice panel lift}}{qS} \right)$
C_D	drag coefficient $\left(\frac{\text{Twice panel drag}}{qS} \right)$

C_m	pitching-moment coefficient referred to $0.25\bar{c}$ $\left(\frac{\text{Twice panel pitching moment}}{qS\bar{c}} \right)$
C_B	bending-moment coefficient at plane of symmetry $\left(\frac{\text{Root bending moment}}{q \left(\frac{S}{2} \right) \left(\frac{b}{2} \right)} \right)$
q	effective dynamic pressure over span of model, pounds per square foot $\left(\frac{1}{2} \rho V^2 \right)$
S	twice wing area of semispan model, 0.1250 square foot
\bar{c}	mean aerodynamic chord of wing, 0.181 foot; based on relationship $\frac{2}{S} \int_0^{b/2} c^2 dy$ (using theoretical tip)
c	local wing chord
b	twice span of semispan model
y	spanwise distance from plane of symmetry
ρ	air density, slugs per cubic foot
V	airspeed, feet per second
M	effective Mach number over span of model
M_a	average chordwise local Mach number
M_l	local Mach number
R	Reynolds number of wing based on \bar{c}
α	angle of attack, degrees
ϵ	effective downwash angle, degrees
q_{wake}/q	ratio of point dynamic pressure at the quarter chord of the tail mean aerodynamic chord to free-stream dynamic pressure

- $(L/D)_{\max}$ maximum ratio of lift to drag
- $y_{c.p.}$ lateral center of pressure, percent semispan $(100C_B/C_L)$
- h_t tail height relative to wing chord plane extended, percent semispan, positive for tail positions above chord plane extended

TESTS

The tests were made in the Langley high-speed 7- by 10-foot tunnel utilizing an adaptation of the NACA wing-flow technique for obtaining transonic speeds. The technique used involves placing the model in the high-velocity flow field generated over the curved surface of a bump on the tunnel floor. (See reference 2.)

Typical contours of local Mach number in the vicinity of the model location on the bump obtained from surveys with no model in position are shown in figure 5. It is seen that there is a Mach number gradient of about 0.04 over the model semispan at low Mach numbers and from 0.06 to 0.07 at the highest Mach numbers. The chordwise Mach number gradient is generally less than 0.01. No attempt has been made to evaluate the effects of this chordwise and spanwise Mach number gradient. Note that the long dashed lines shown near the root of the wing (fig. 5) indicate a local Mach number 5 percent below the maximum value and represent a nominal extent of the bump boundary layer. The effective test Mach number was obtained from contour charts similar to those presented in figure 5 using the relationship

$$M = \frac{2}{S} \int_0^{b/2} cM_a dy$$

The variation of mean test Reynolds number with Mach number is shown in figure 6. The boundaries on the figure are an indication of the probable range in Reynolds number caused by variations in test conditions in the course of the investigation.

Force and moment data, effective downwash angles, and the ratio of dynamic pressure at 25 percent of the tail mean aerodynamic chord to free-stream dynamic pressure were obtained for various model configurations through a Mach number range of 0.60 to 1.18 and an angle-of-attack range of -2° to 10° .

No tares have been applied to the data to account for the presence of the end plates on the models. Jet-boundary corrections have not been evaluated because the boundary conditions to be satisfied are not rigorously defined. However, inasmuch as the effective flow field is large compared with the span and chord of the model the corrections are believed to be small.

By measuring tail floating angles without a model installed it was determined that a tail spacing of 2 inches would produce negligible interference effects of reflected shock waves on the tail floating angles. Downwash angles for the wing-alone configuration were therefore obtained simultaneously for the middle, highest, and lowest tail positions in one series of tests and simultaneously for the two intermediate positions in succeeding runs. (See fig. 3.) For the wing-fuselage tests the effective downwash angles at the chord plane extended were determined by mounting a free-floating tail on the center line of the fuselage. The downwash angles presented are increments from the tail floating angles without a model in position. It should be noted that the floating angles measured are in reality a measure of the angle of zero pitching moment about the tail pivot axis rather than the angle of zero lift. It has been estimated, however, that for the tail arrangement used a downwash gradient of 2° across the span of the tail will result in an error of less than 0.2° in the measured downwash angle.

Total-head readings obtained from the tail survey comb have been corrected for bow wave loss. The static-pressure values used in computing the dynamic-pressure ratios were obtained by use of a static probe with no model in position.

RESULTS AND DISCUSSION

A table of the figures presenting the results is given as follows:

	Figure
Wing-alone force data	7
Wing-fuselage force data	8
Effective downwash angles (wing alone)	9
Effective downwash angles (wing fuselage)	10
Downwash gradients	11
Dynamic-pressure surveys	12
Summary of aerodynamic characteristics	13

The discussion is based on the summarized values given in figure 13 unless otherwise noted. Note that the slopes summarized in figure 13 have been averaged over a lift-coefficient range of ± 0.1 of the nominal lift coefficient.

Lift and Drag Characteristics

The isolated wing lift-curve slope measured near zero lift was about 0.066 at a Mach number of 0.60. (See fig. 7.) This compares with a value of 0.063 estimated for this Mach number by use of the charts in reference 3. In the Mach number range between 0.85 and 0.98 it appears that the maximum lift coefficient may be fairly close to 0.6 (fig. 7). The basic lift-curve slope was increased by an average of about 9 percent by the addition of the fuselage.

The drag rise at zero lift (fig. 13) began at a Mach number of about 0.89 for both the wing and wing-fuselage configurations. It is interesting to note that although this drag rise occurred at a Mach number about 0.04 lower than for the 45° sweptback wing (reference 1), which, except for sweepback, had geometric characteristics identical to those of the present wing, the values of $C_{D_{L=0}}$ and $(L/D)_{\max}$ at the highest Mach numbers are not materially different for the two models. The absolute drag coefficients are probably high because of the presence of end-plate tares and the relatively low Reynolds numbers at which these tests were made.

The lateral center of pressure for the wing alone ($C_L = 0.4$) was located at 44 percent of the semispan at a Mach number of 0.6. This value compared with an estimated low-speed value of about 45 percent semispan (reference 3). Between $M = 0.9$ and 1.00 there was a fairly abrupt movement of $y_{c.p.}$ to about 50 percent semispan. This same outboard shift was obtained with the 45° sweptback wing at a somewhat higher Mach number. (See reference 1.) The addition of the fuselage generally moved $y_{c.p.}$ inboard approximately 3 percent of the semispan.

Pitching-Moment Characteristics

Near zero lift the wing-alone aerodynamic center was located at 27 percent of the mean aerodynamic chord $\left(\frac{\partial C_M}{\partial C_L} \right)_M = -0.02$ up to $M = 0.80$. This value compares with an estimated low-speed aerodynamic-center location of 24 percent \bar{c} (reference 3). The addition of the fuselage moved the aerodynamic center forward about 2 percent \bar{c} at the low Mach numbers.

At $C_L = 0.4$ the wing-alone aerodynamic center was about 25 percent \bar{c} at low Mach numbers and moved back to 46 percent \bar{c} at the highest Mach numbers. The destabilizing effect of the fuselage was slightly more pronounced at $C_L = 0.4$ than at $C_L = 0$.

Downwash and Dynamic-Pressure Surveys

The variation of effective downwash angle with tail height and angle of attack for the wing alone and wing-fuselage at various Mach numbers is presented in figures 9 and 10. The downwash gradient $\partial\epsilon/\partial\alpha$ near zero lift for the wing alone (fig. 11) increased as the tail location approached the chord plane, at Mach numbers below 1.00. Above $M = 1.00$ $\partial\epsilon/\partial\alpha$ was maximum at a tail location of 30 percent semispan below the chord plane. At the higher lift coefficients $\partial\epsilon/\partial\alpha$ was generally less than the zero lift value for tail positions below the chord plane and was higher for tail positions above the chord plane.

The addition of the fuselage caused a marked increase in $\partial\epsilon/\partial\alpha$ for tail positions near the chord plane (figs. 10 and 11) up to $M = 0.95$. Above $M = 1.00$ the effect of the fuselage on the downwash gradient near the chord plane was small. Note that the test angle-of-attack range with the free-floating tails nearest the chord line extended was restricted because of the presence of the fuselage.

The results of point dynamic-pressure surveys made in a vertical plane containing the 25-percent mean-aerodynamic-chord point of the free-floating tails used in the downwash surveys are presented in figure 12. The maximum loss in dynamic pressure at the wake center line for the higher angles of attack was never more than 15 percent of the free-stream dynamic pressure.

The addition of the fuselage showed practically no effect on the dynamic-pressure ratios throughout most of the Mach number range. At 10° angle of attack at the higher Mach numbers the addition of the fuselage shifted the wake center line above that of the wing alone.

The dynamic-pressure surveys show that for the particular tail length used a tail position of 10 percent of the semispan or more below the chord plane would generally be most favorably located from consideration of wake effects.

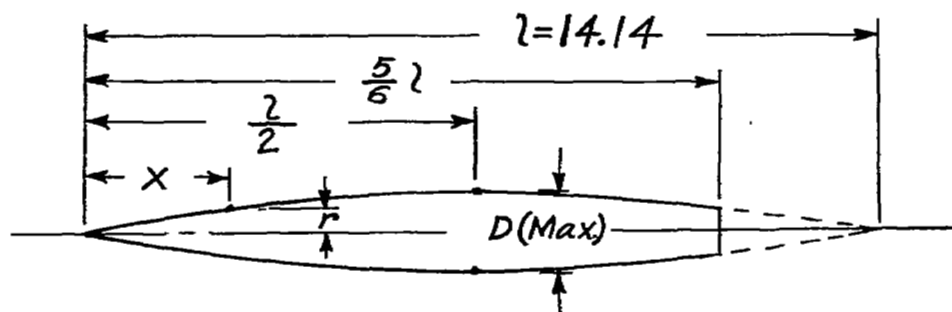
Langley Aeronautical Laboratory
National Advisory Committee for Aeronautics
Langley Air Force Base, Va.

REFERENCES

1. Weil, Joseph, and Goodson, Kenneth W.: Aerodynamic Characteristics of a Wing with Quarter-Chord Line Swept Back 45° , Aspect Ratio 4, Taper Ratio 0.6, and NACA 65A006 Airfoil Section. Transonic-Bump Method. NACA RM No. L9A21, 1949.
2. Schneider, Leslie E., and Ziff, Howard L.: Preliminary Investigation of Spoiler Lateral Control on a 42° Sweptback Wing at Transonic Speeds. NACA RM No. L7F19, 1947.
3. DeYoung, John: Theoretical Additional Span Loading Characteristics of Wings with Arbitrary Sweep, Aspect Ratio, and Taper Ratio. NACA TN No. 1491, 1947.

TABLE I.- FUSELAGE ORDINATES

[Basic fineness ratio 12; actual fineness ratio 10
achieved by cutting off the rear one-sixth of
the body; $\bar{c}/4$ located at $l/2$]



Ordinates			
x/l	r/l	x/l	r/l
0	0	0	0
.005	.00231	.4500	.04143
.0075	.00298	.5000	.04167
.0125	.00428	.5500	.04130
.0250	.00722	.6000	.04024
.0500	.01205	.6500	.03842
.0750	.01613	.7000	.03562
.1000	.01971	.7500	.03128
.1500	.02593	.8000	.02526
.2000	.03090	.8338	.02000
.2500	.03465	.8500	.01852
.3000	.03741	.9000	.01125
.3500	.03933	.9500	.00439
.4000	.04063	1.0000	0
L. E. radius = 0.00057			



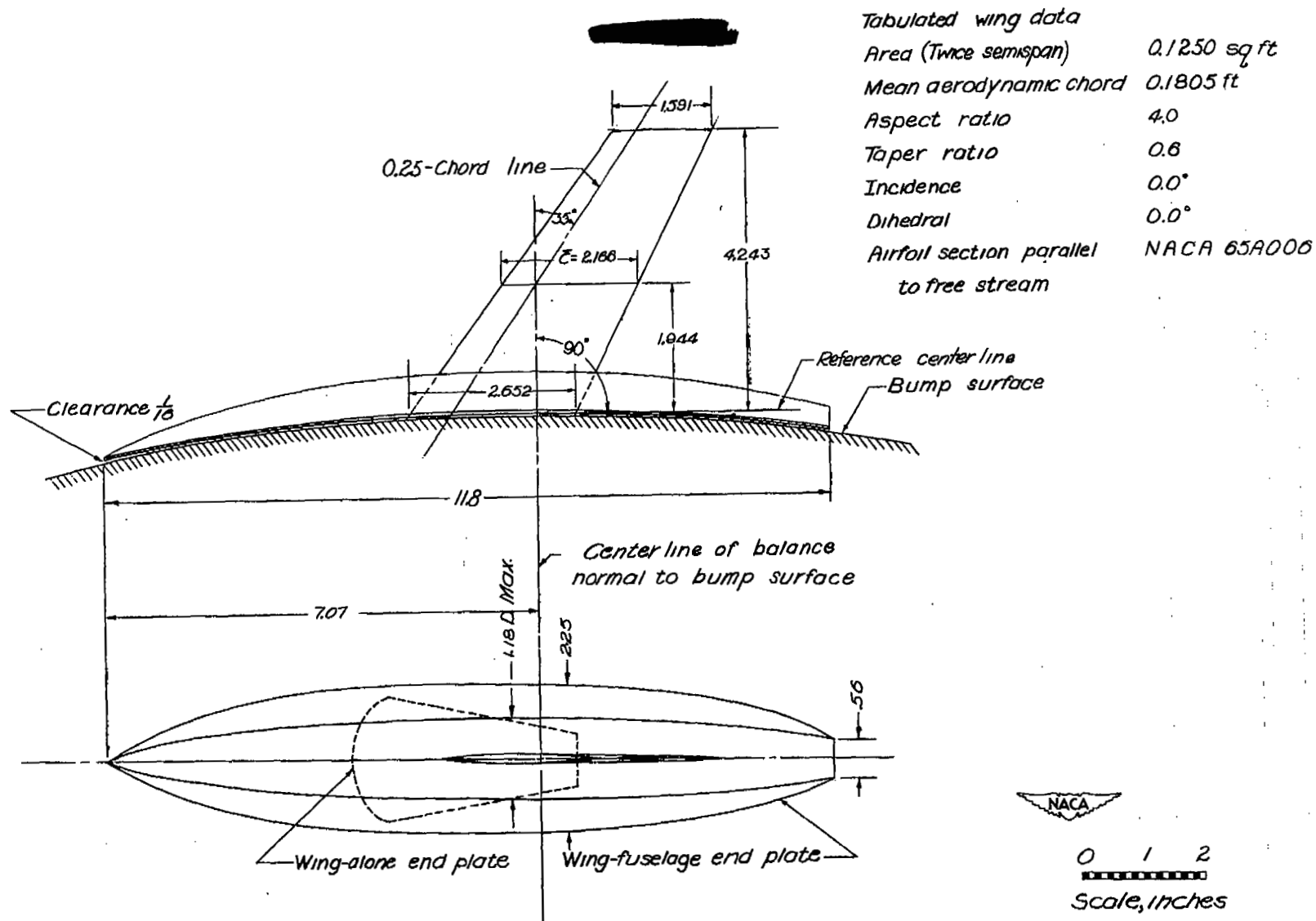


Figure 1.— General arrangement of a model with 35° sweptback wing, aspect ratio 4, taper ratio 0.6, and NACA 65A006 airfoil.

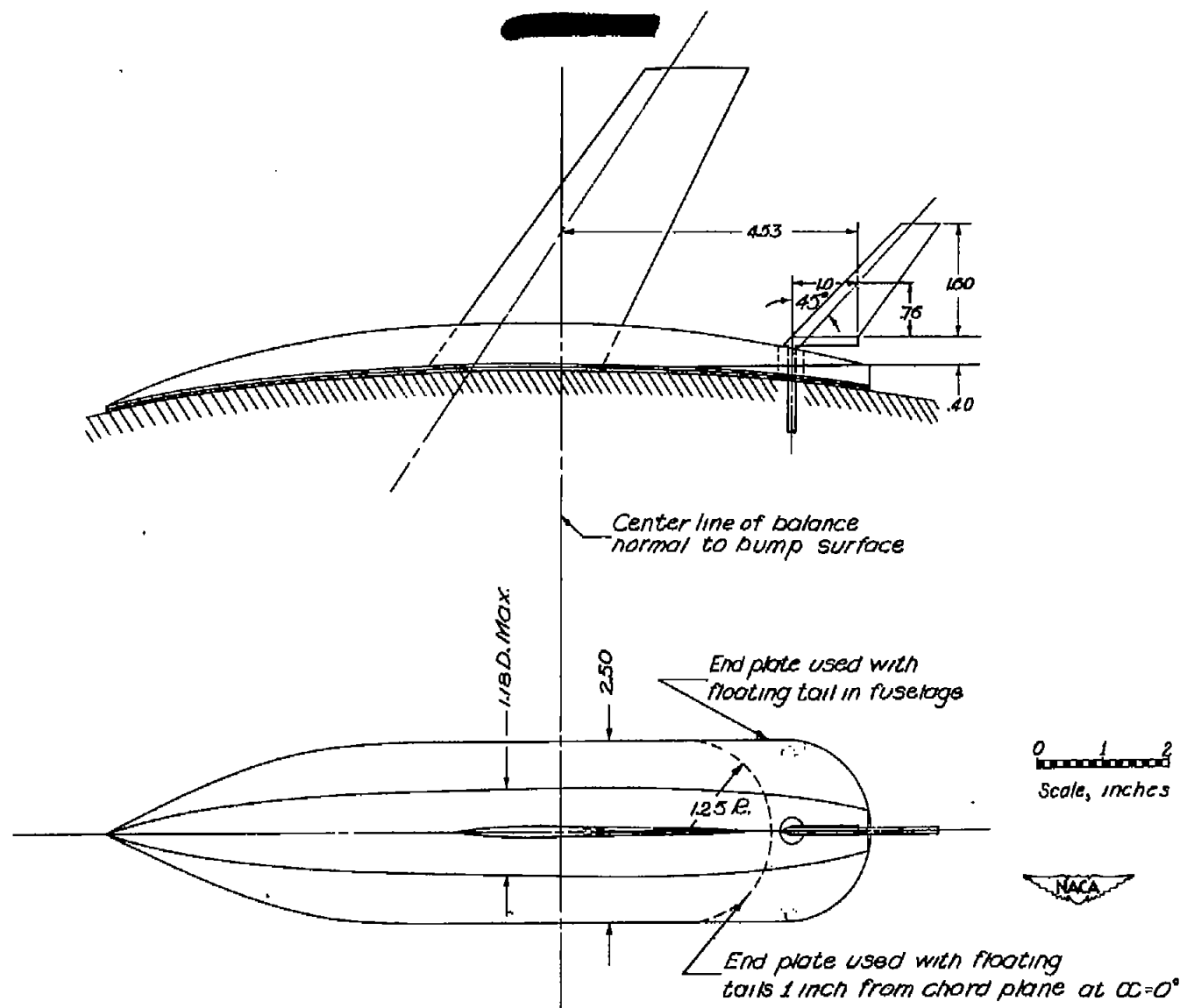


Figure 2.- Details of free-floating tail mounted in fuselage of a model with 35° sweptback wing, aspect ratio 4, taper ratio 0.6, and NACA 65A006 airfoil.

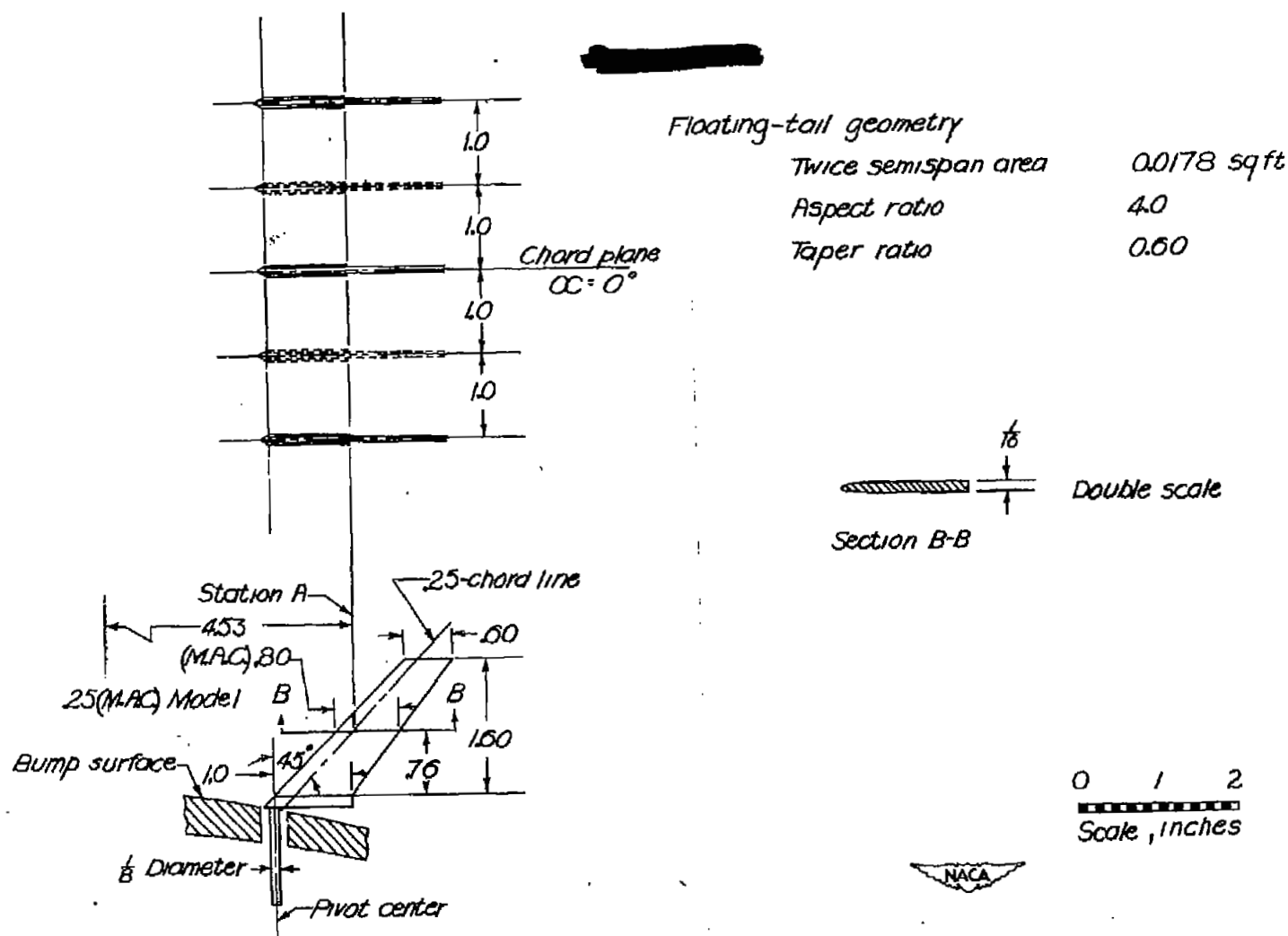


Figure 3.— Details of free-floating tails used in surveys behind a model with 35° sweptback wing, aspect ratio 4, taper ratio 0.6, and NACA 65A006 airfoil.

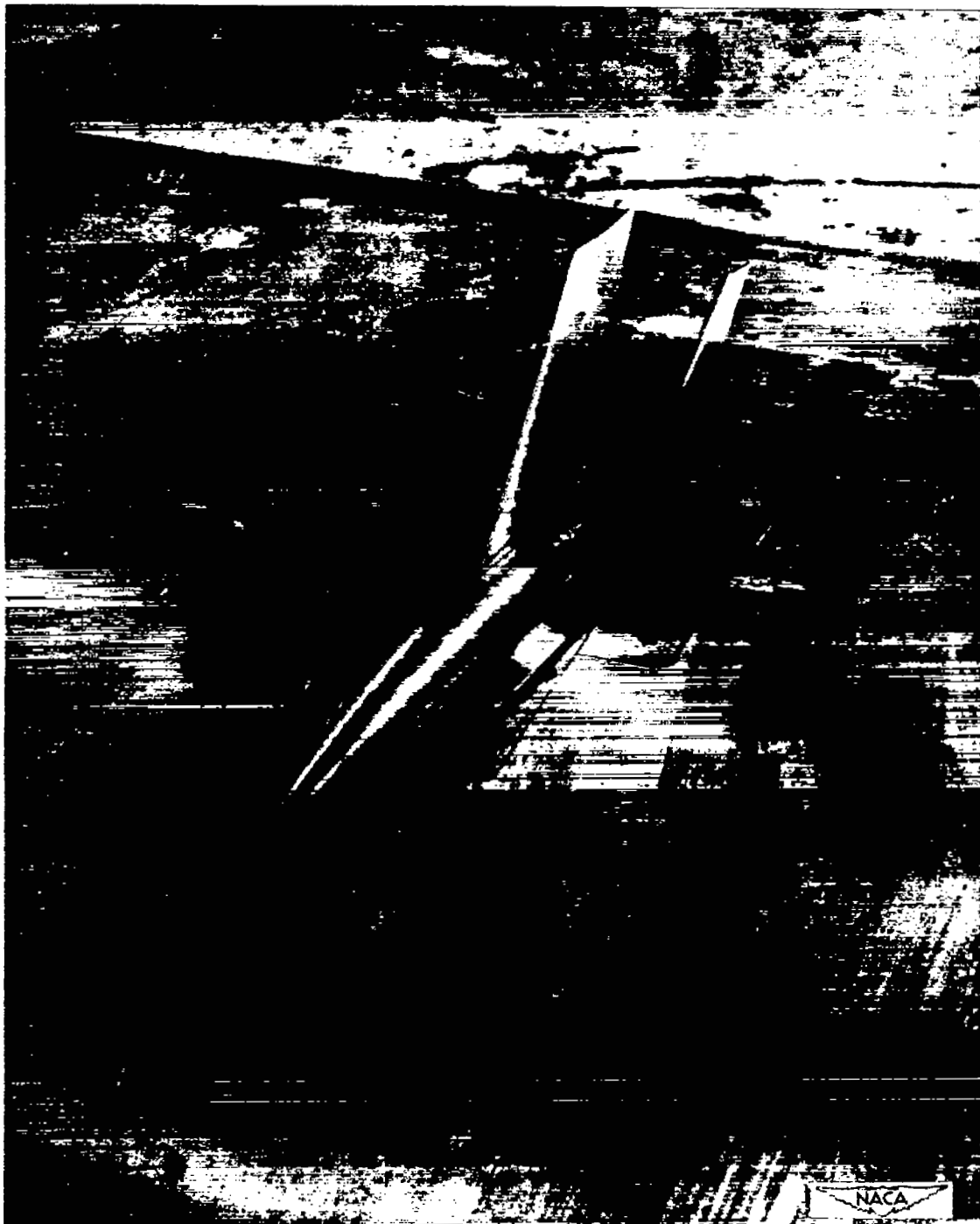


Figure 4.— Photograph of a model with 35° sweptback wing, aspect ratio 4, taper ratio 0.6, and NACA 65A006 airfoil showing free-floating tail mounted in fuselage.

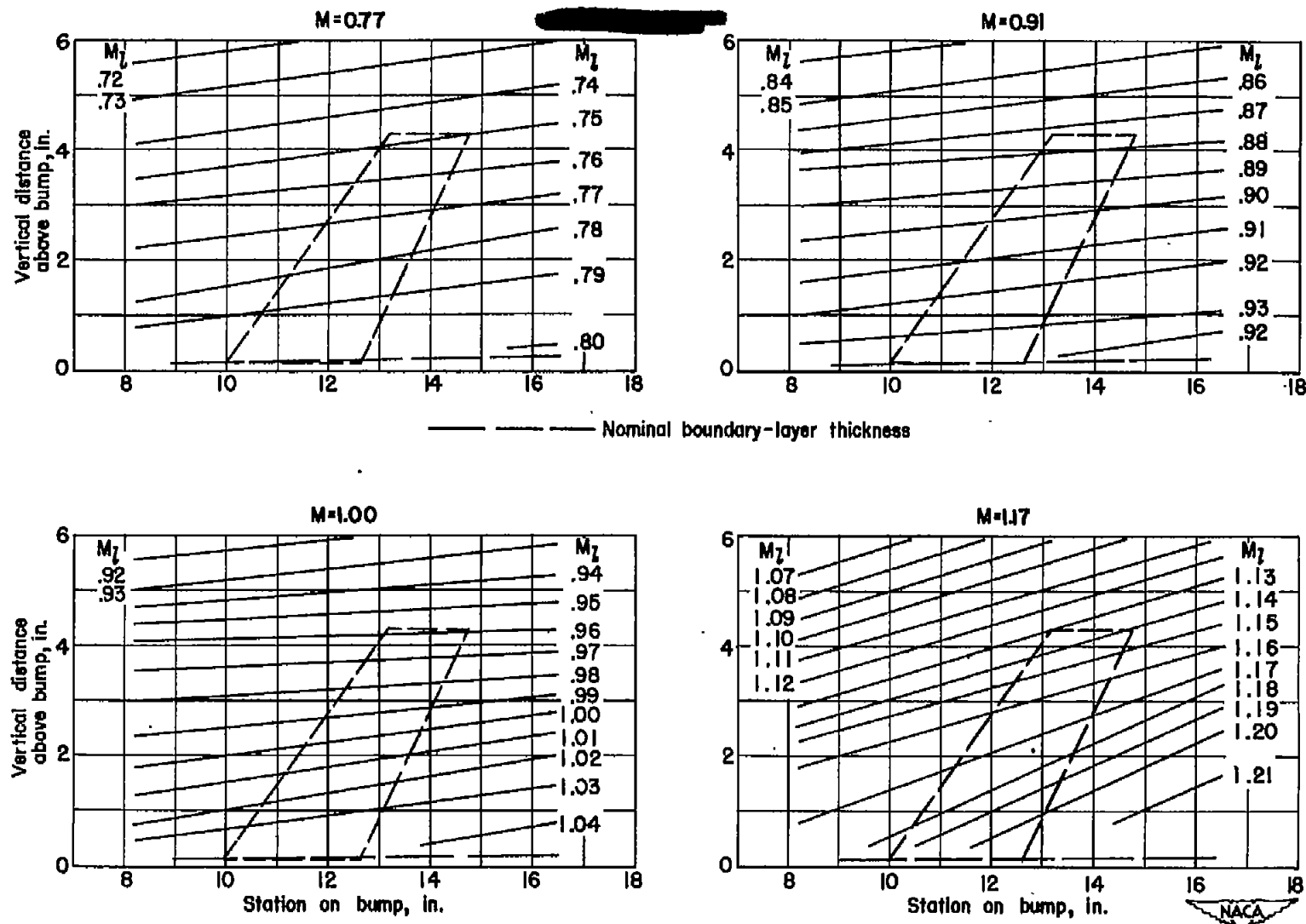


Figure 5.- Typical Mach number contours over transonic bump in region of model location.

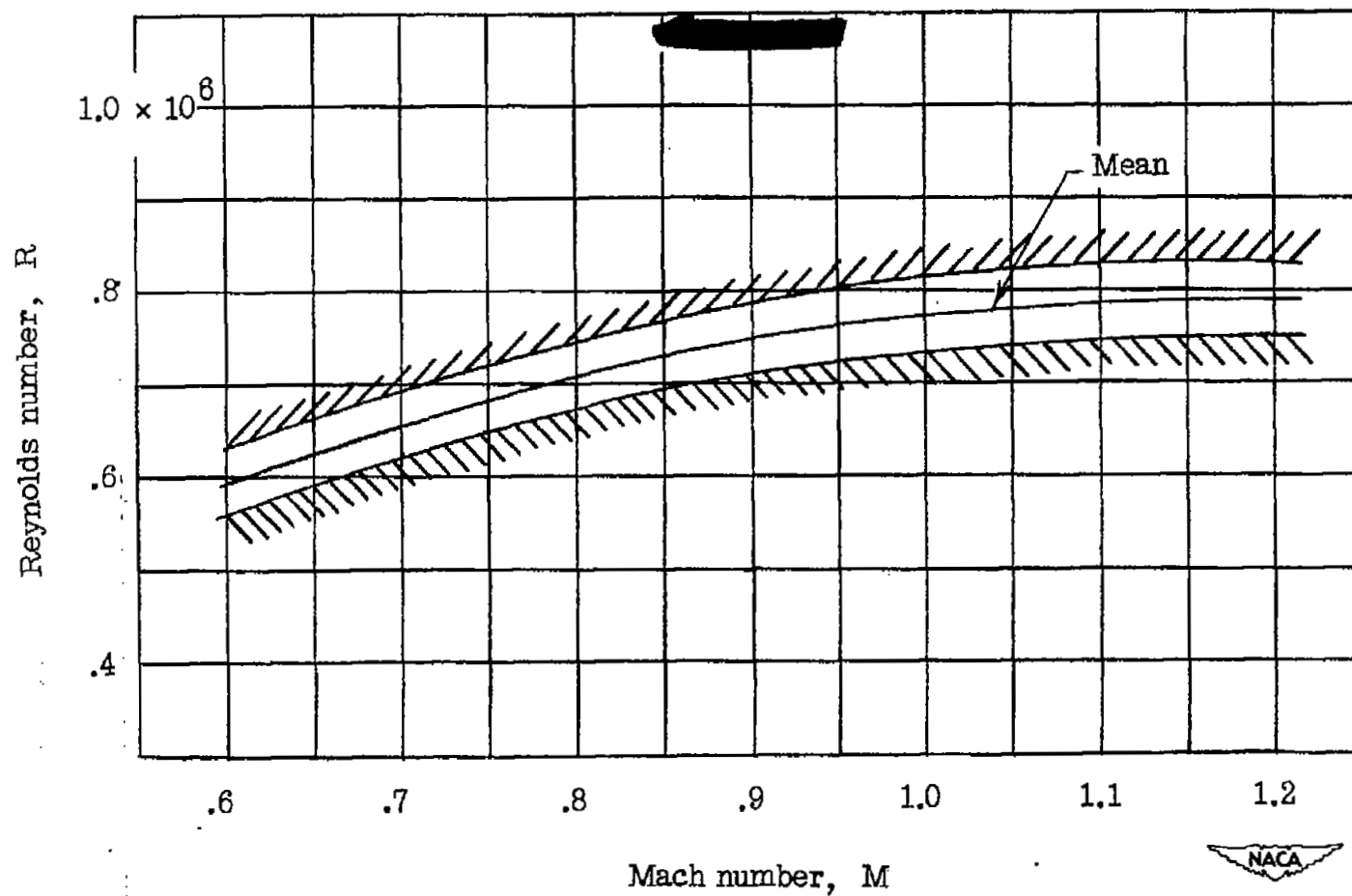


Figure 6.— Variation of test Reynolds number with Mach number for a model with 35° sweptback wing, aspect ratio 4, taper ratio 0.6, and NACA 65A006 airfoil.

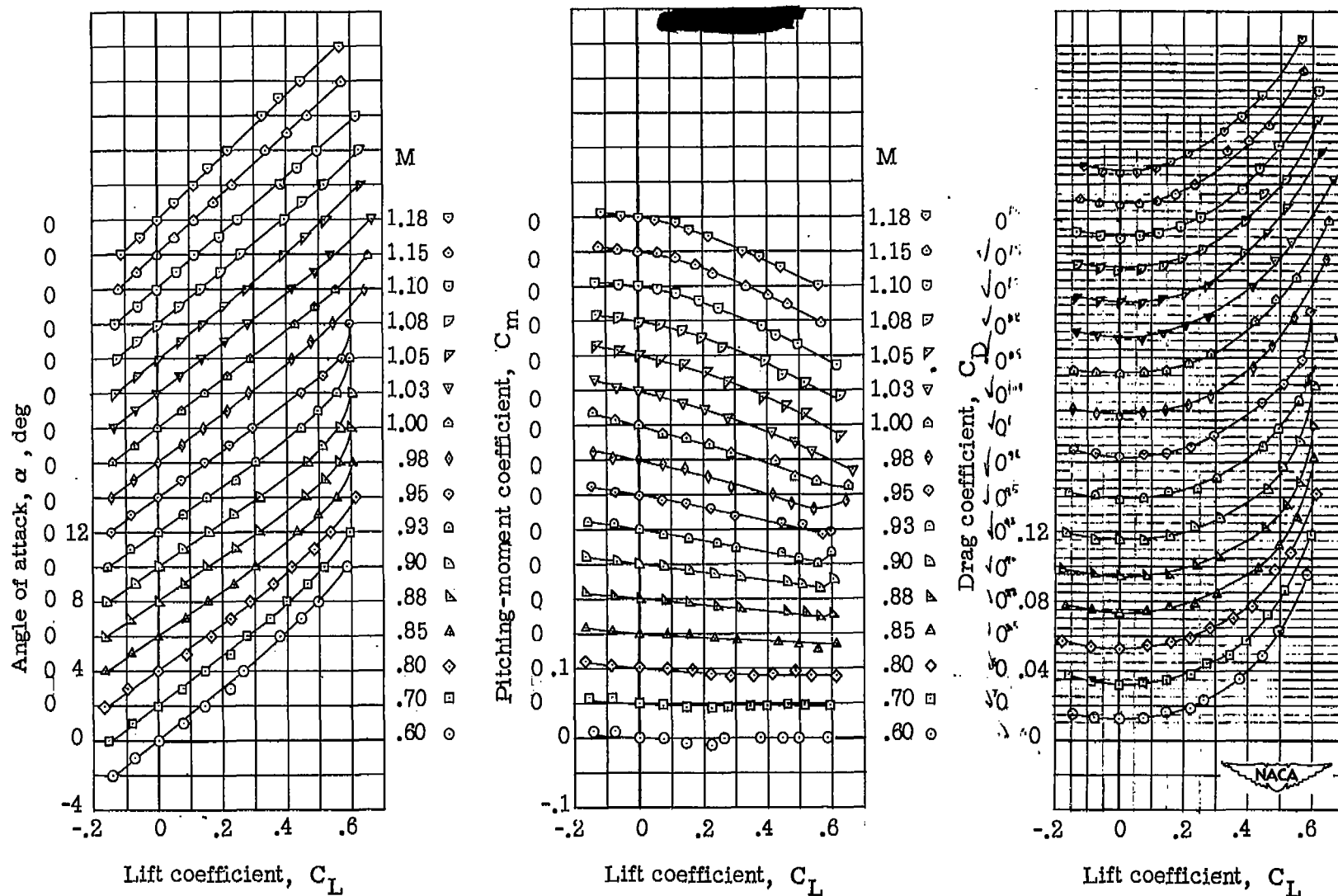


Figure 7.- Wing-alone aerodynamic characteristics for a model with 35° sweptback wing, aspect ratio 4, taper ratio 0.6, and NACA 65A006 airfoil.

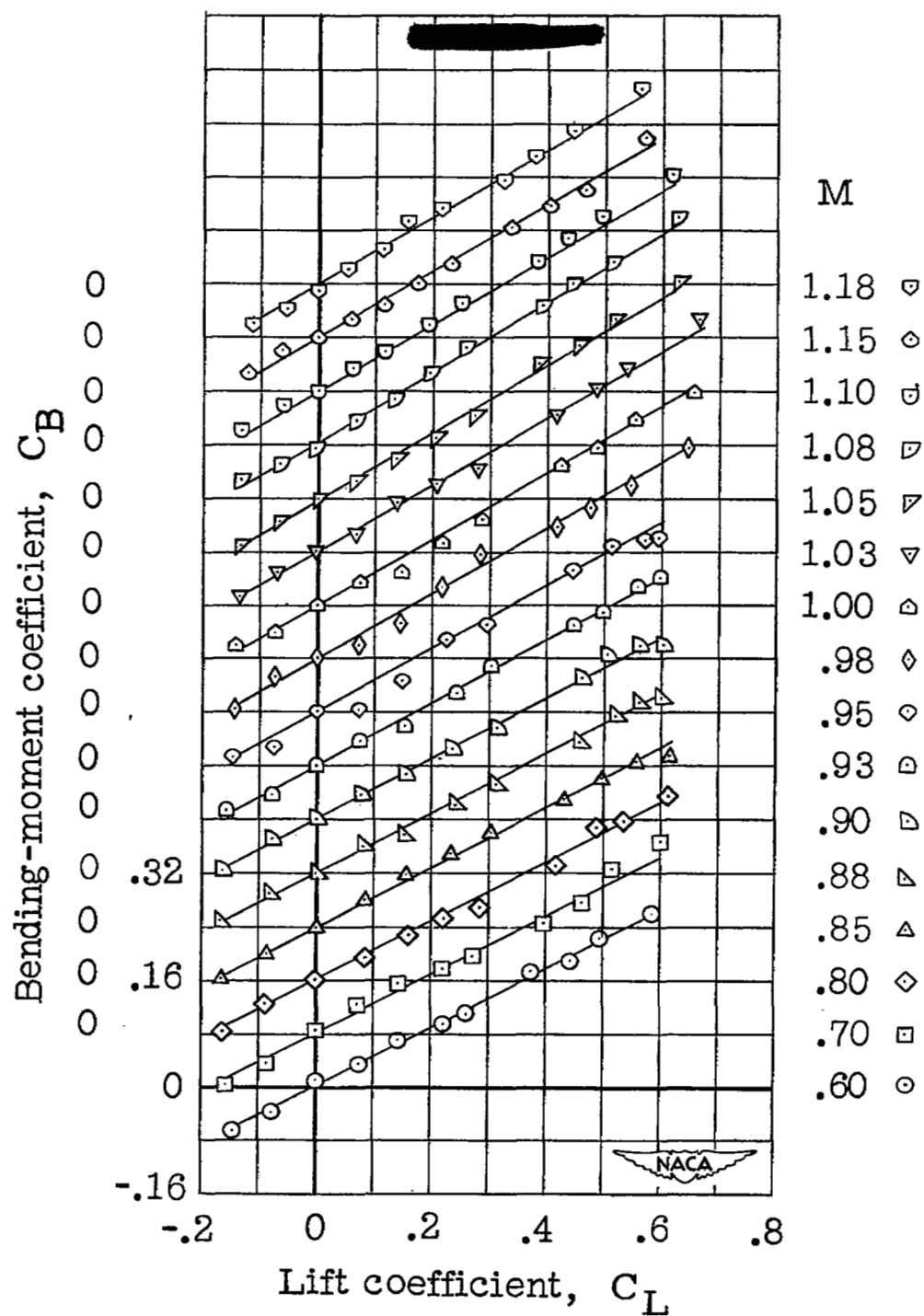


Figure 7.- Concluded.

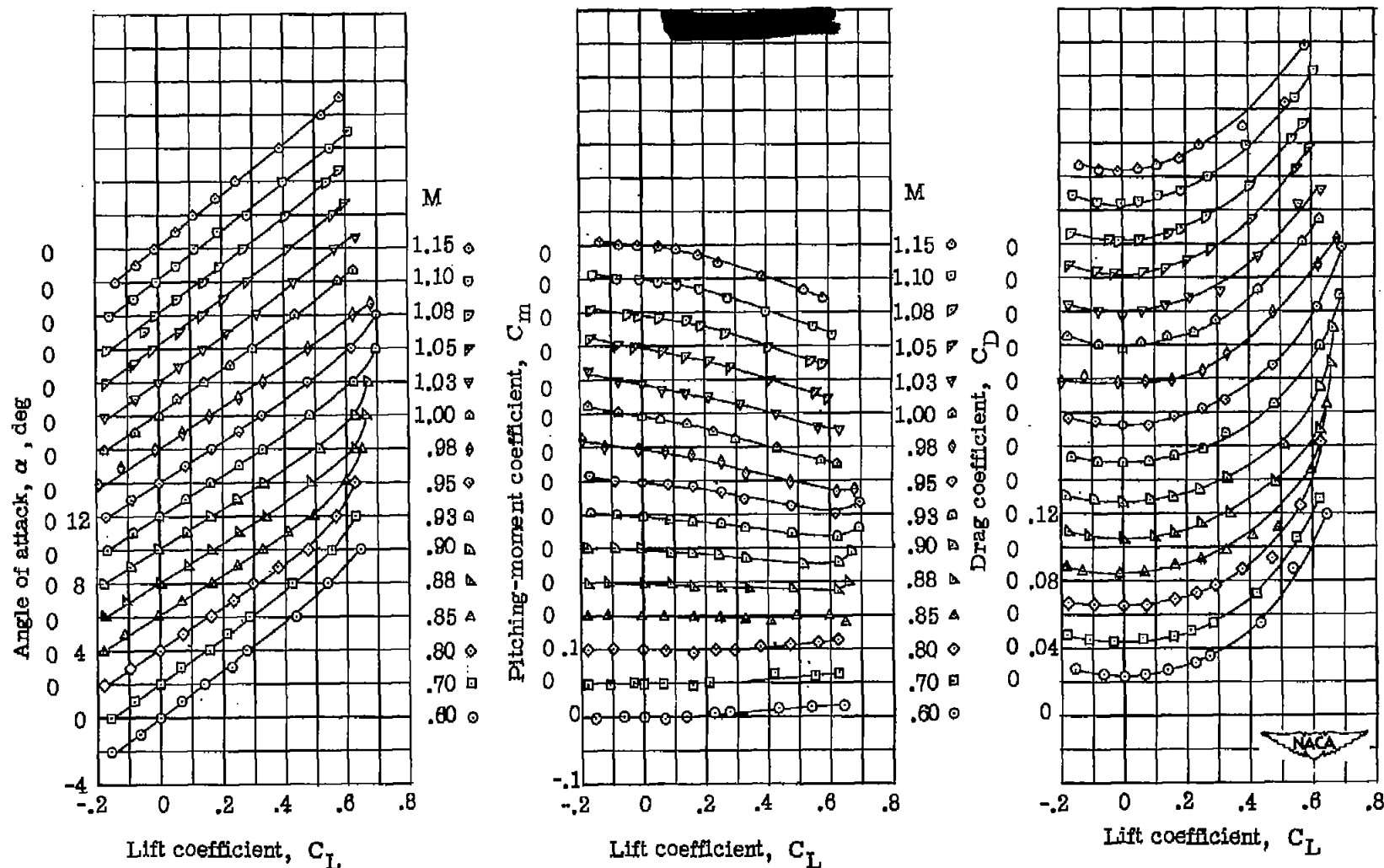


Figure 8.- Wing-fuselage aerodynamic characteristics for a model with 35° sweptback wing, aspect ratio 4, taper ratio 0.6, and NACA 65A006 airfoil.

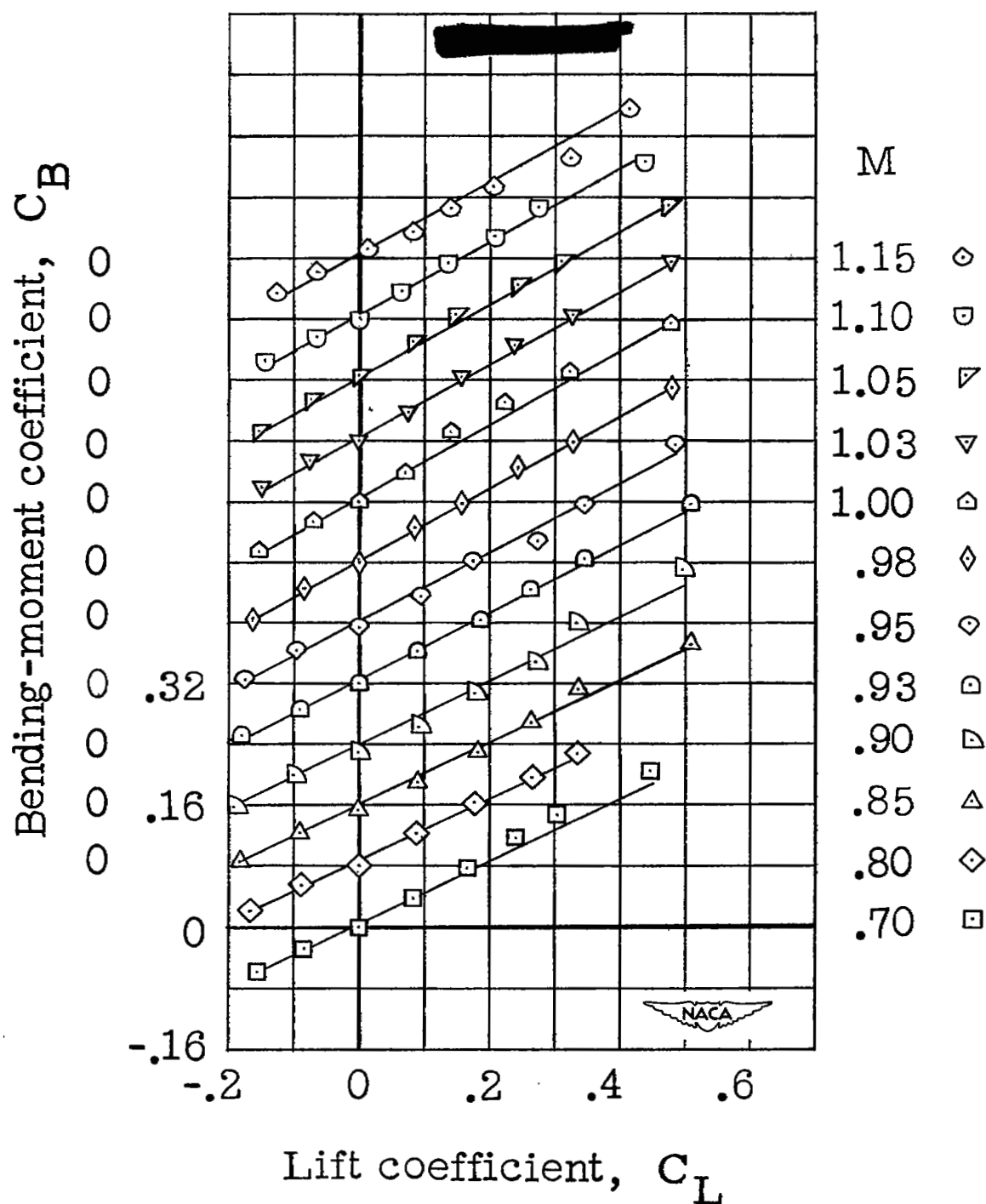


Figure 8.— Concluded.

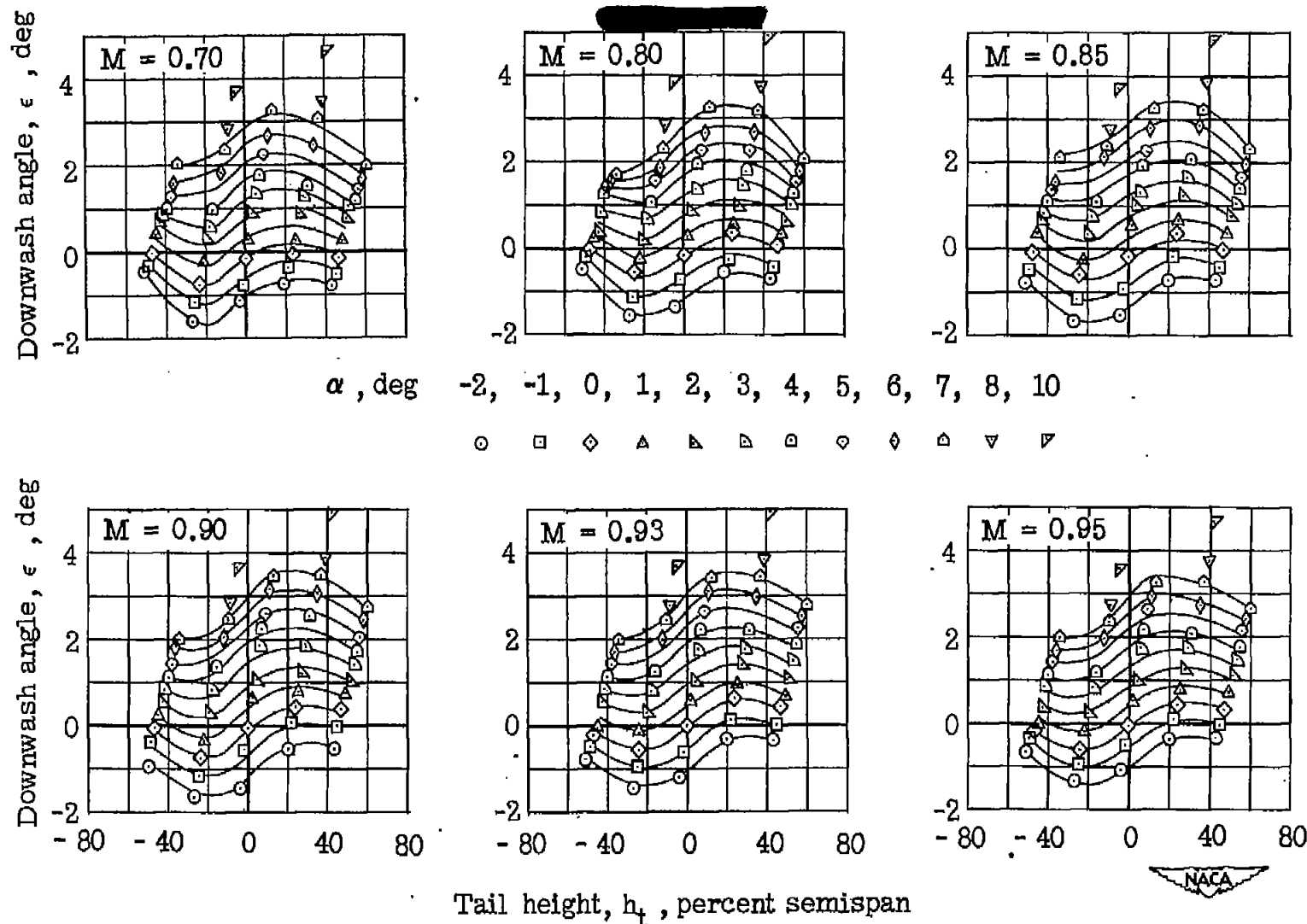


Figure 9.— Effective downwash angles in region of tail plane for a model with 35° sweptback wing, aspect ratio 4, taper ratio 0.6, and NACA 65A006 airfoil. Wing alone.

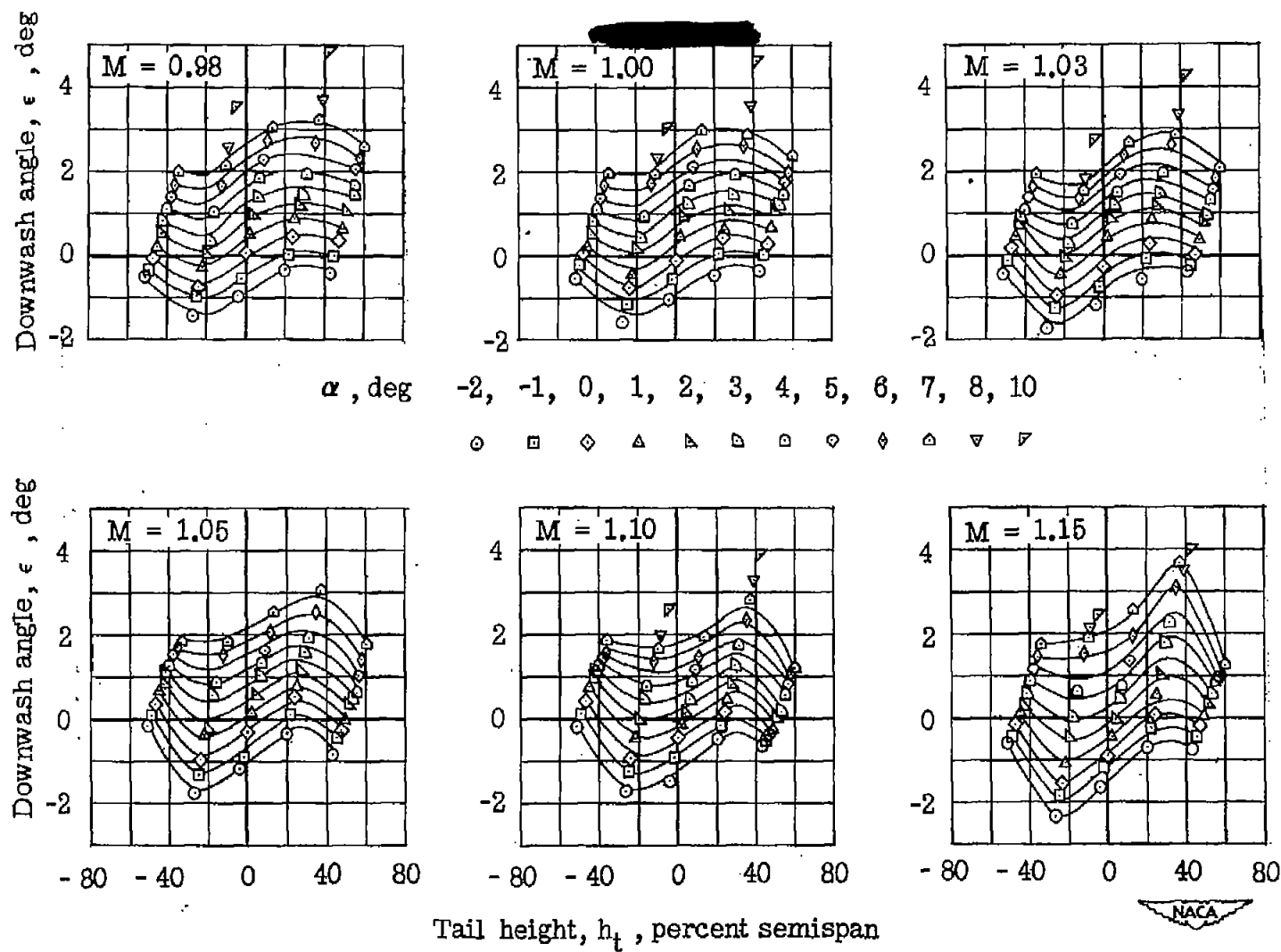


Figure 9.- Concluded.

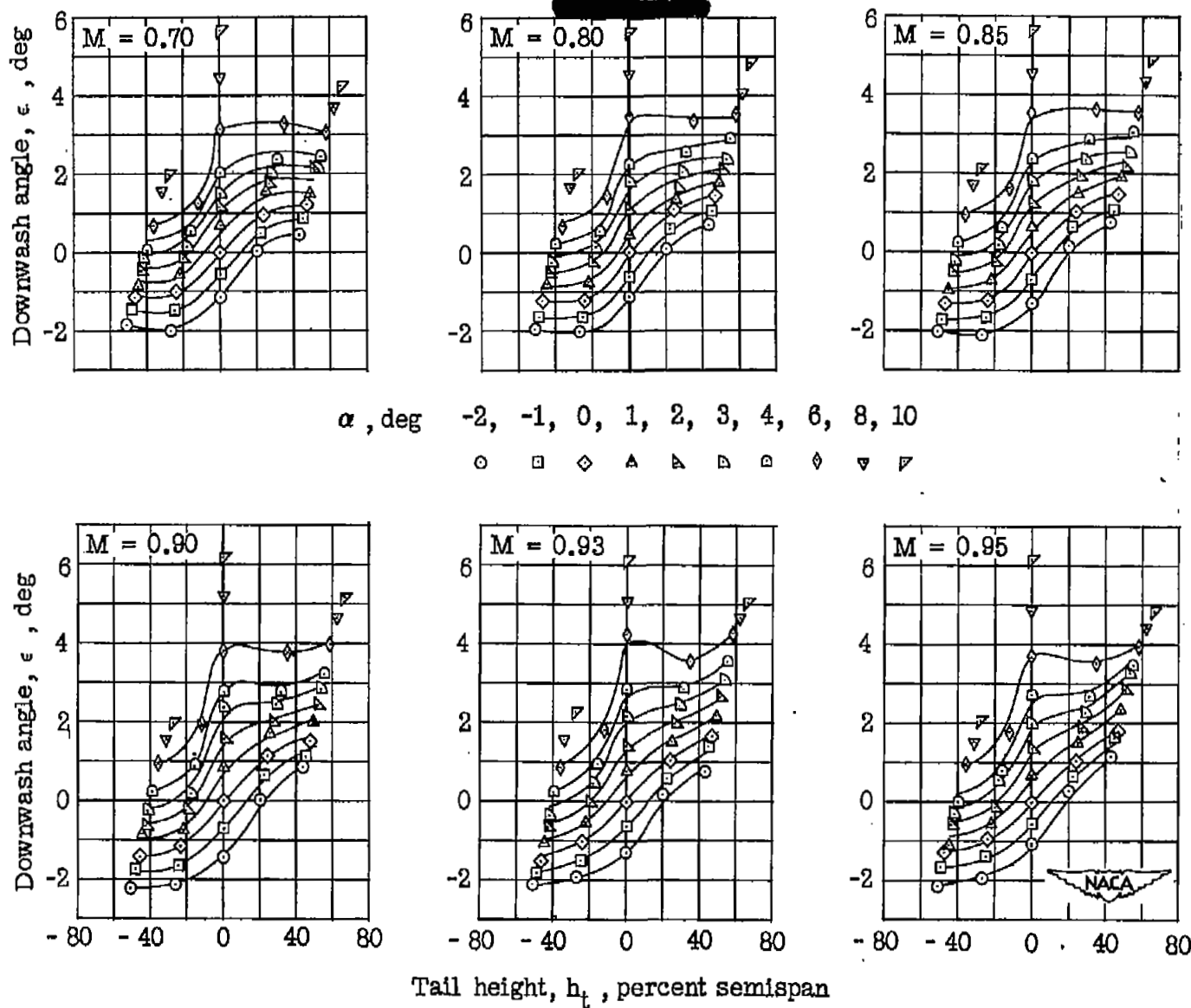
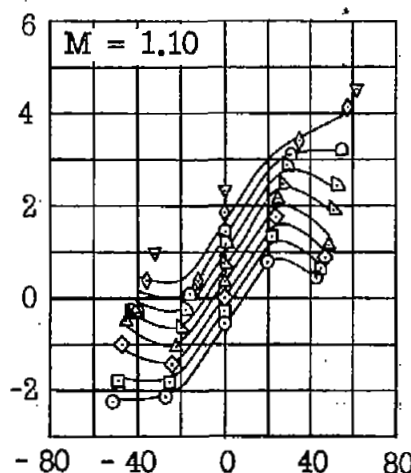
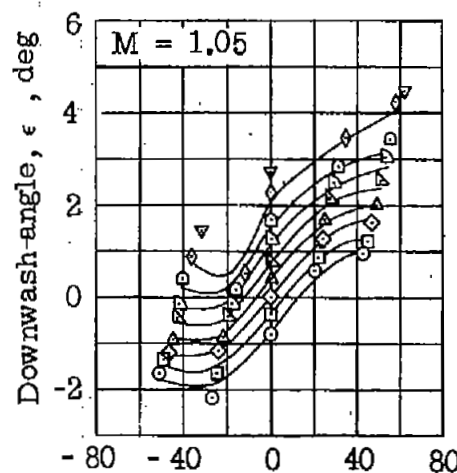
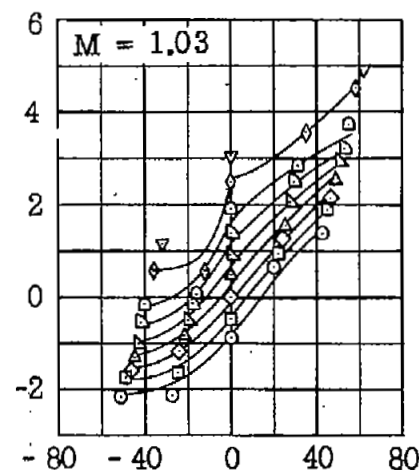
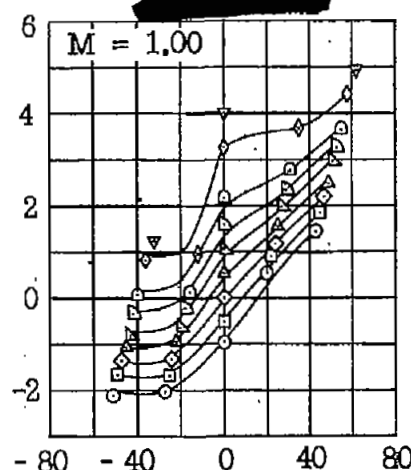
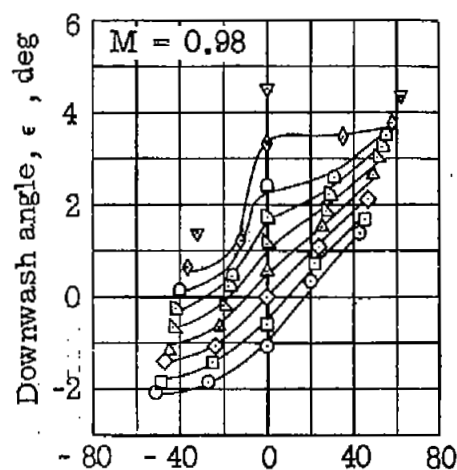


Figure 10.- Effective downwash angles in region of tail plane for a model with 35° sweptback wing, aspect ratio 4, taper ratio 0.6, and NACA 65A006 airfoil. Wing-fuselage.



α , deg

- 2 ○
- 1 □
- 0 ◇
- 1 ▲
- 2 ▴
- 3 ▽
- 4 ▢
- 6 ◆
- 8 ▼



Tail height, h_t , percent semispan

Figure 10.- Concluded.

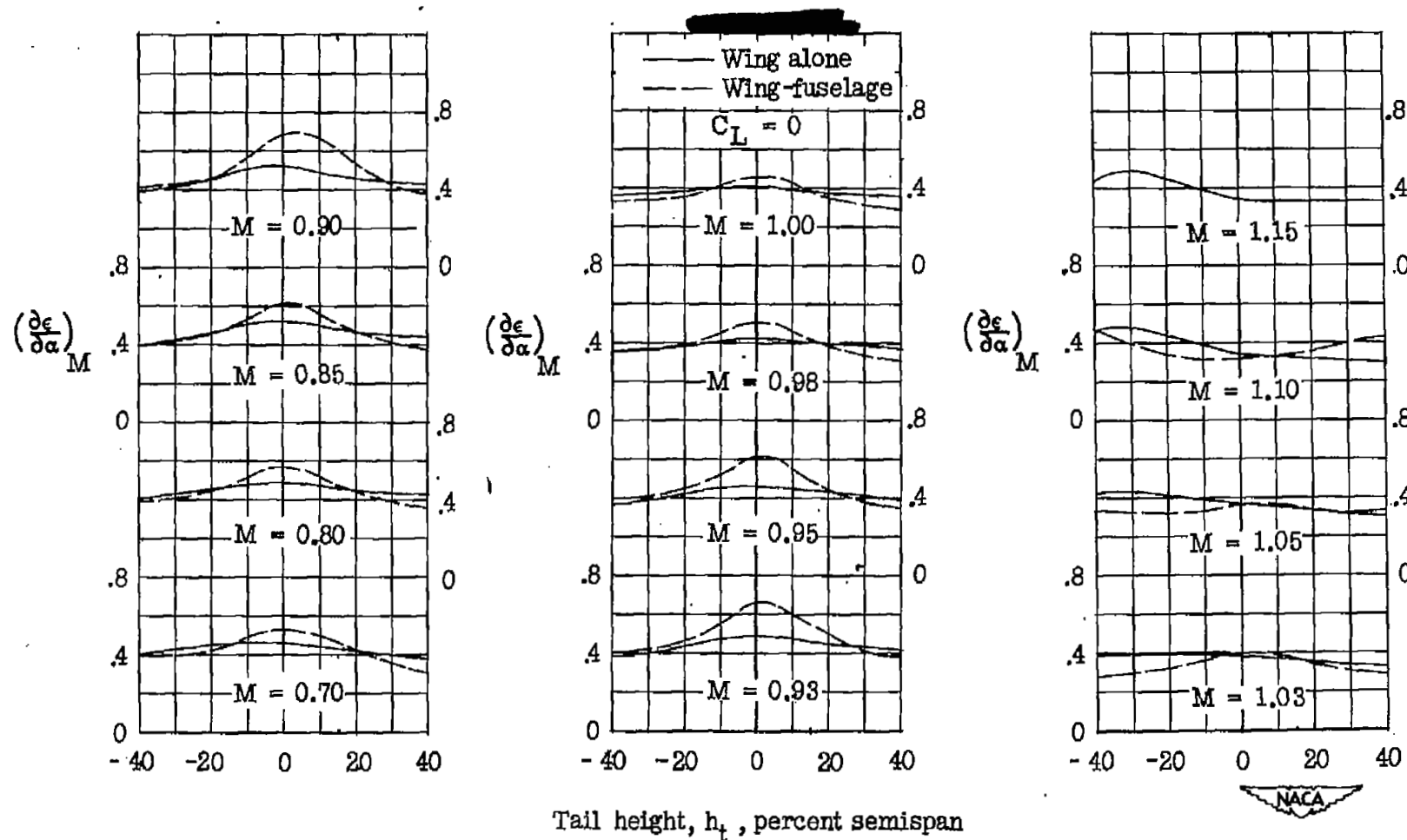


Figure 11.— Variation of downwash gradient with tail height and Mach number for a model with 35° sweptback wing, aspect ratio 4, taper ratio 0.6, and NACA 65A006 airfoil.

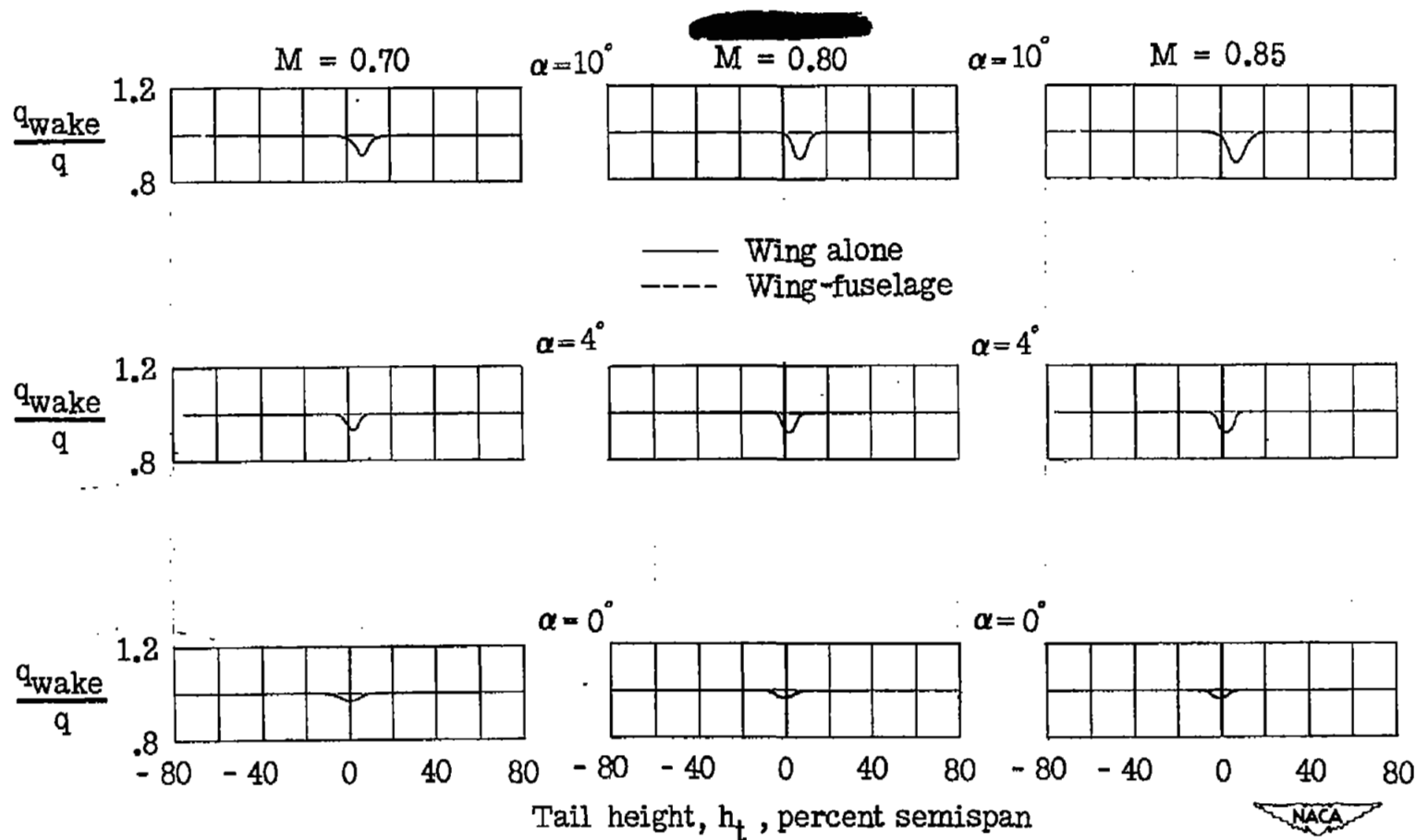


Figure 12.— Dynamic-pressure surveys in region of tail plane for a model with 35° sweptback wing, aspect ratio 4, taper ratio 0.6, and NACA 65A006 airfoil.

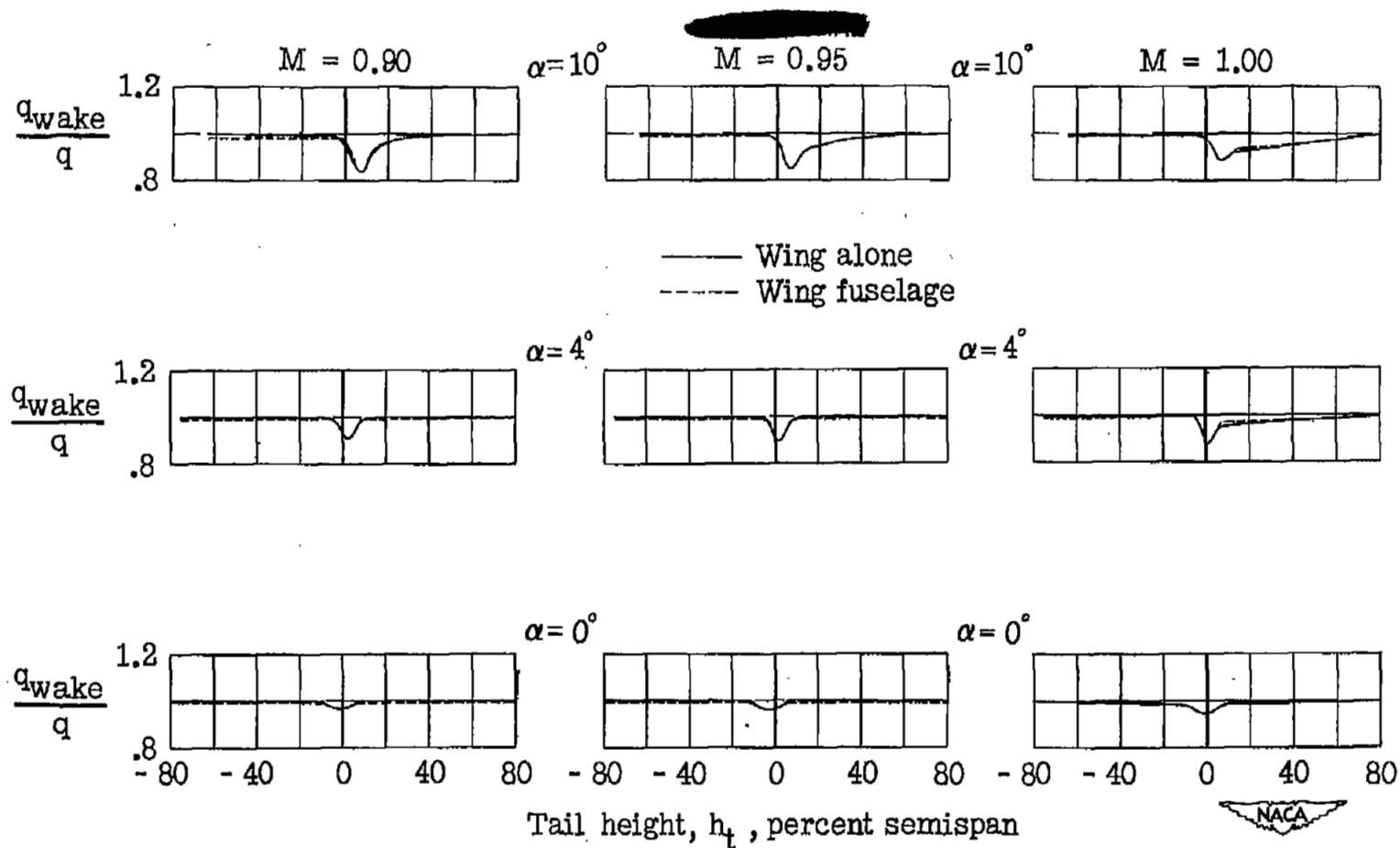


Figure 12.- Continued.

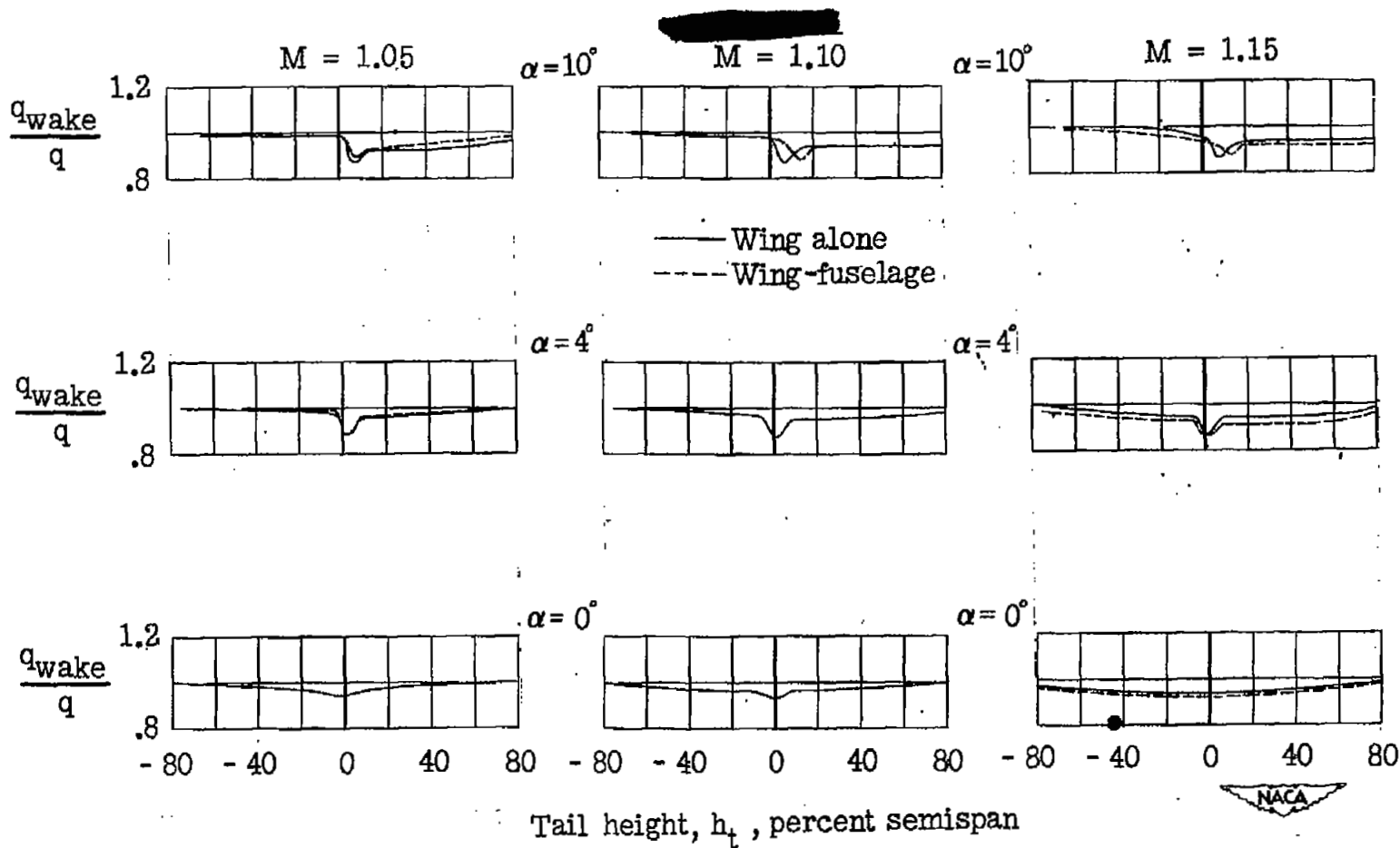


Figure 12, - Concluded.

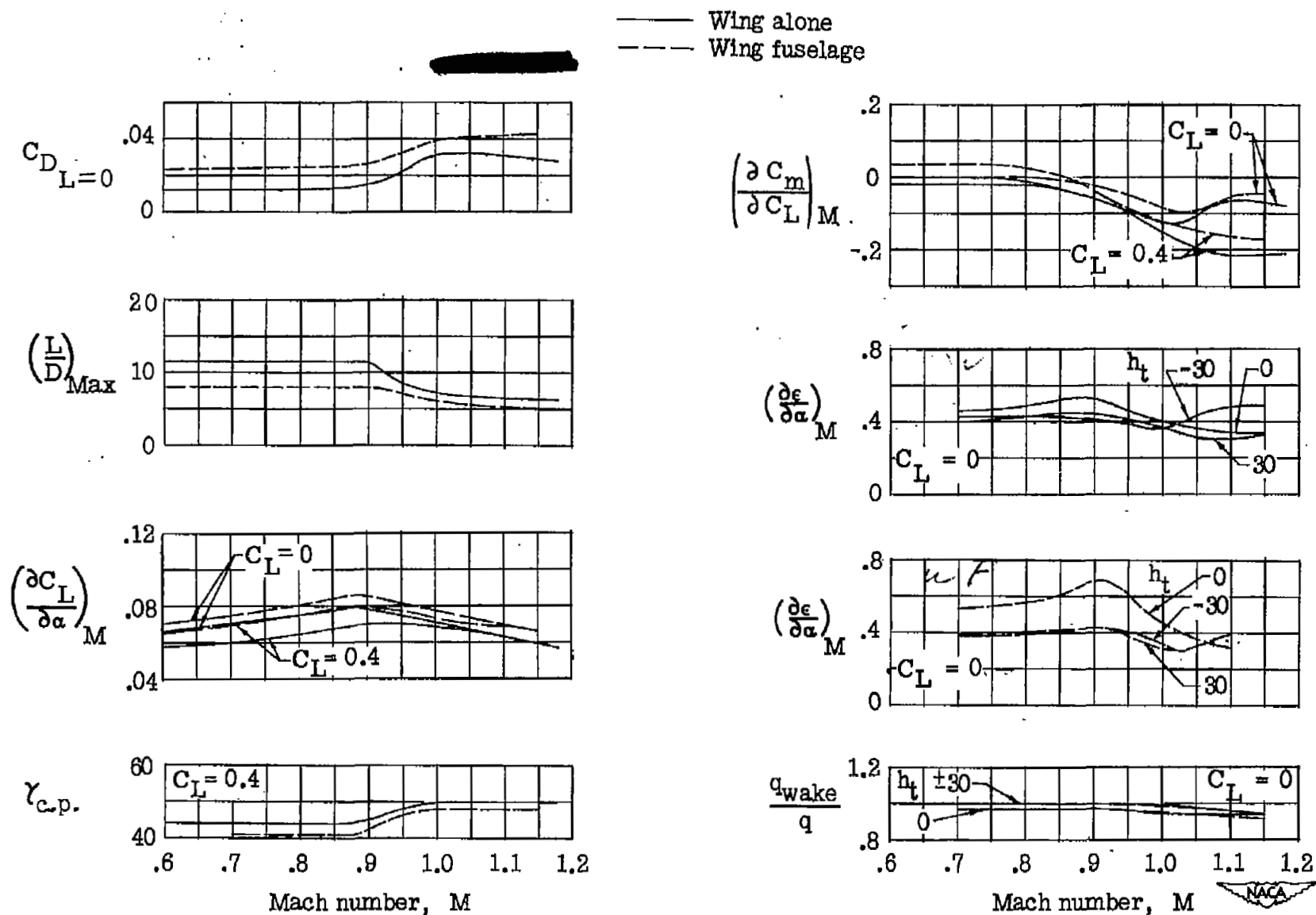


Figure 13.— Summary of aerodynamic characteristics for a model with 35° sweptback wing, aspect ratio 4, taper ratio 0.6, and NACA 65A006 airfoil.

NASA Technical Library



3 1176 01436 7214